Citation
Li, Z. and Chen, W. and Hao, H. 2018. Blast mitigation performance of cladding using square dome-shape kirigami folded structure as core. International Journal of Mechanical Sciences. 145: pp. 83-95. http://doi.org/10.1016/j.ijmecsci.2018.06.035

Blast mitigation performance of cladding using Square Dome-shape Kirigami folded structure as core

Zhejian Li[1], Wensu Chen[1]*, Hong Hao[1,2]*

[1]*Centre for Infrastructural Monitoring and Protection*
School of Civil and Mechanical Engineering, Curtin University, Australia
Kent Street, Bentley, WA 6102, Australia
[2]*School of Civil Engineering, Guangzhou University, China*

*corresponding author

Abstract

Structural response of the sacrificial cladding with Square Dome-shape Kirigami (SDK) structure as core under blast loads is investigated in this study. A sample of SDK core folded from a pre-cut aluminium sheet is crushed under quasi-static loading condition. A numerical model is then developed and calibrated using experimental data. The calibrated model of SDK foldcore cladding is then placed on to a rigid block as a sacrificial layer to resist blast loading for structure protection. To evaluate the blast mitigation capacities, the parameters such as peak load transmitted to the protected structure, energy absorption, center crushed distance and loading duration are compared among the claddings with different cores. Compared to square honeycomb, superior performance of blast mitigation is demonstrated for the proposed SDK foldcore sacrificial cladding by yielding a uniform collapsing similar to aluminium foam. Significant increase in energy absorption of the core is observed for the sacrificial cladding with SDK foldcore. It also yields a higher plateau stress than aluminium foam of the same density and is applicable to a wider range of blast loadings. The peak transmitted load to the protected structure is reduced by more than 70% comparing with the case without cladding. SDOF analysis of the sacrificial cladding systems is carried out and validated using numerical results. Based on the SDOF analysis, complete solution is derived and then used to obtain simplified design charts to show the suitable range of blast load scenarios where the sacrificial claddings are effective.

1. Introduction

Sandwich structures are widely used in many applications, such as vehicle, aircraft, ship, packaging and structural protections owing to the characteristics of light weight and high energy absorption capacities [1]. Recently, sandwich structures have also been used as energy absorber in different impact or blast protective applications. Sacrificial cladding, in particular, has been investigated extensively both numerically and experimentally. Sacrificial cladding usually consists of a crushable core sandwiched by two skins and is fixed onto the protected structure. By allowing large deformation of the core under a constant low stress, it absorbs large amount of energy and reduces the load transmitted to the protected structure in the event of blast [2]. Many topologies of the core were developed, including lattices [3], polymeric foams [4], aluminium honeycomb [5, 6], metallic foams [2, 7], auxetic core [8, 9] and load-self-canceling core [10-13].

Folded structure was originally proposed by Miura in 1972 [14]. Miura-type origami core is folded from an un-broken sheet material along the creases without stretching or twisting of the faces. It was initially used as packaged solar panel for space deployment [15]. Miura-type origami folded structure was recently used as core of sandwich structure for its advantages such as continuous manufacturing and open channel design to reduce heat and humidity inside the core [16, 17]. However, its crushing resistance and energy absorption capacities were not as comparable as honeycomb with similar density [18-20]. Kirigami foldcore was developed to allow the sheet material to be cut or stamped prior to folding, therefore, achieving more complex geometries and higher crushing resistance capacity. Up to 74% increase in average crushing stress is shown for cube strip kirigami foldcore than the standard Miura-type origami foldcore and comparable crushing resistance with square honeycomb is demonstrated [19].

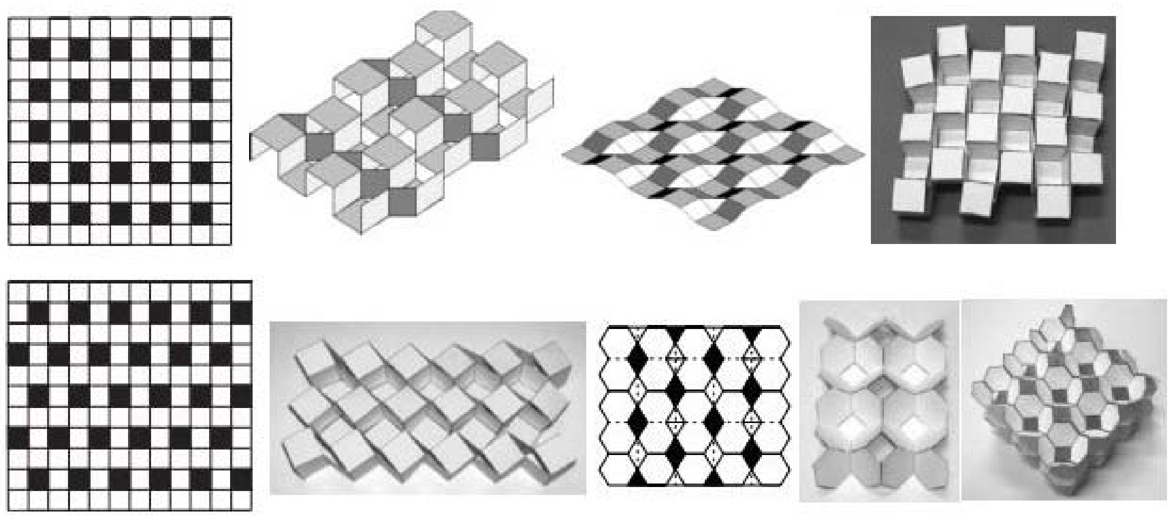

Figure 1. Examples of existing kirigami structure, black shades are the cut out of sheet material [21]

In most of the existing kirigami foldcore designs, the adjacent vertical faces are not connected, as shown in Figure 1. Higher crushing resistance and energy absorption are expected for the foldcore with connected adjacent vertical faces, as more constraints can be provided during the out-of-plane crushing of the foldcore. A Square Dome Kirigami (SDK) foldcore with adjacent vertical faces connected is therefore proposed and crushing behavior of this new foldcore is investigated under quasi-static and dynamic out-of-plane crushing [22, 23]. Uniform crushing resistance with low ratio of peak to average crushing stress is demonstrated for the proposed SDK foldcore. Furthermore, consistent crushing behavior is also observed under various crushing speeds, as compared with the honeycomb and cube strip kirigami structure. These aluminium foam-like characteristics of SDK foldcore indicate its potential applications in structures for energy absorption, such as core for sacrificial cladding against blast loading [24, 25].

In this study, the performance of cladding with SDK foldcore subjected to blast loading is investigated through intensive numerical simulations. For comparison, the responses of square honeycomb and aluminium foam of the same density subjected to the same loading conditions are also simulated. The numerical model is firstly calibrated using the quasi-static crushing testing data of SDK foldcore. The model is then used to simulate structural response of claddings under blast loading. Different blast intensities are considered. Criteria including energy absorption by cladding core and the peak load transmitted to the protected structure are used to evaluate the performance among these claddings. In addition, Single Degree of Freedom (SDOF) analysis is applied to develop a simplified design procedure and guideline for estimating the required height of SDK foldcore sacrificial cladding under specific blast loading scenarios.

2. Model validation

Folding configurations and dimensions of the SDK foldcore are shown in Figure 2. As mentioned previously, the inclined sidewalls are connected with adjacent faces in both sides via triangular connections as shown in Figure 2. Small folding gaps of 0.5 mm near the corners of the unit cell are considered in numerical models. Because of the existence of the interconnections between sidewalls, the geometry of the foldcore is determined by three parameters only, i.e. the length of bottom and top edges, a, b and the height of the core H (the parameters are illustrated in Figure 2). Other parameters can be expressed by a, b, H as follows:

$$c = \sqrt{(\frac{a-b}{2})^2 + H^2} \tag{1}$$

$$l = \sqrt{(\frac{a-b}{2})^2 + c^2} \tag{2}$$

$$r = \arctan(\frac{2c}{a-b}) \tag{3}$$

$$\alpha = \gamma - \frac{\pi}{4} \tag{4}$$

$$\beta = \arccos(\frac{\sqrt{2}a - \sqrt{2}b}{2l}) \tag{5}$$

$$\mathrm{X} = \frac{\sin\beta \cdot l}{\sin(\pi - \alpha - \beta)} \tag{6}$$

The total surface area for each SDK unit cell is

$$A_{surf} = 4 \cdot \frac{1}{2} c(a+b) + 8 \cdot \frac{1}{2} \sin\alpha \cdot Xl \tag{7}$$

The relative density, or volumetric density can be calculated by

$$\rho_v = \frac{A_{surf} \cdot T}{a^2 H} \tag{8}$$

where T is the thickness of the sheet.

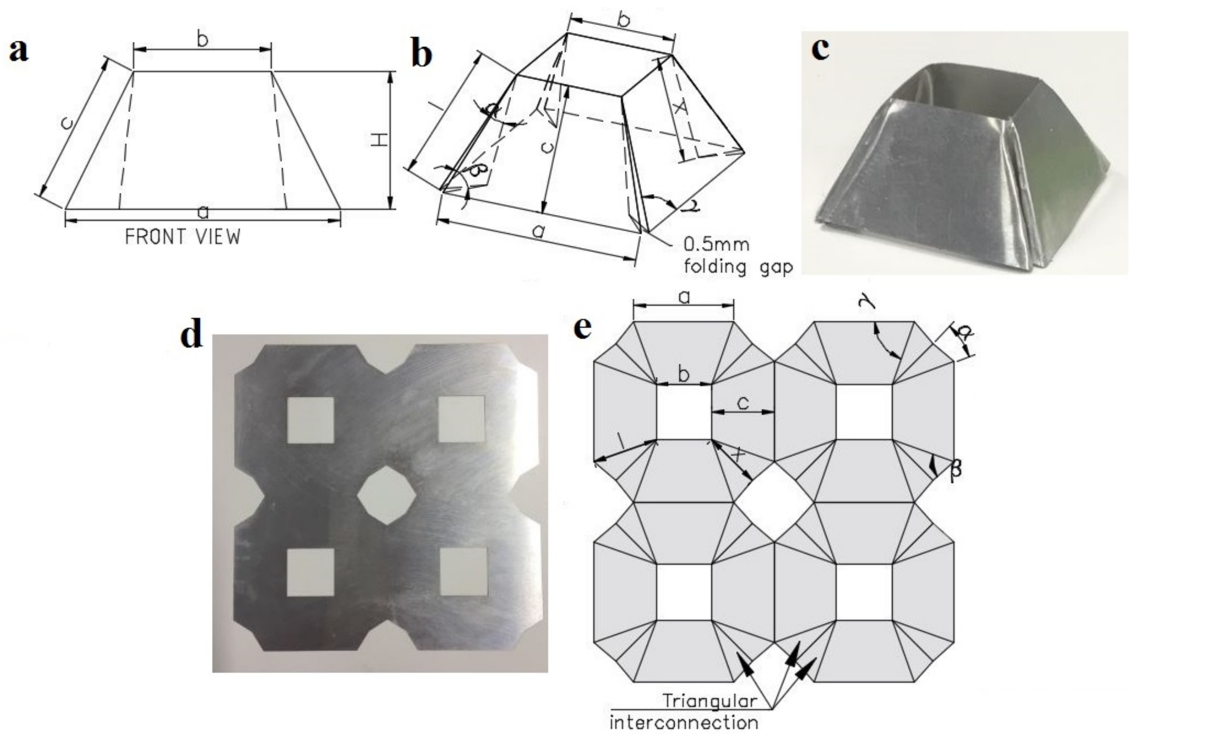

Figure 2. (a) Front view of a SDK foldcore unit cell; (b) isometric view of folding configuration; (c) hand folded single unit prototype; (d) pre-cut aluminium sheet for four-unit sample folding; (e) crease patterns and geometry parameters

2.1 Quasi-static compression test

Hand-fold samples of SDK with four unit cells are crushed under quasi-static compression test with a constant loading rate of 1 mm/min. Due to the availability of the aluminium sheet material, the aluminium sheet with the thickness of 0.26mm is used for the folding the test specimens, which gives a 2.7% relative density for the core. The hand folded sample has a dimension of 83 x 82 x 22 mm, slightly over the designed size of 80 x 80 x 20 mm. This inevitable fabrication inaccuracy is caused by hand folding in preparing these preliminary specimens. As presented in Figure 3 (b), sidewalls of the sample are slightly bent and minor gap can be observed near the bottom edges. These imperfections induced by hand folding are unlikely to be avoided in this early research stage, machine stamping could be developed to eliminate the inaccuracy and reduce the production time. The folded sample is placed onto a steel plate with a 2 mm high boundary strip to constrain the outer edges of foldcore under out-of-plane crushing. No glue or other fixing is applied between the foldcore and the supporting plate.

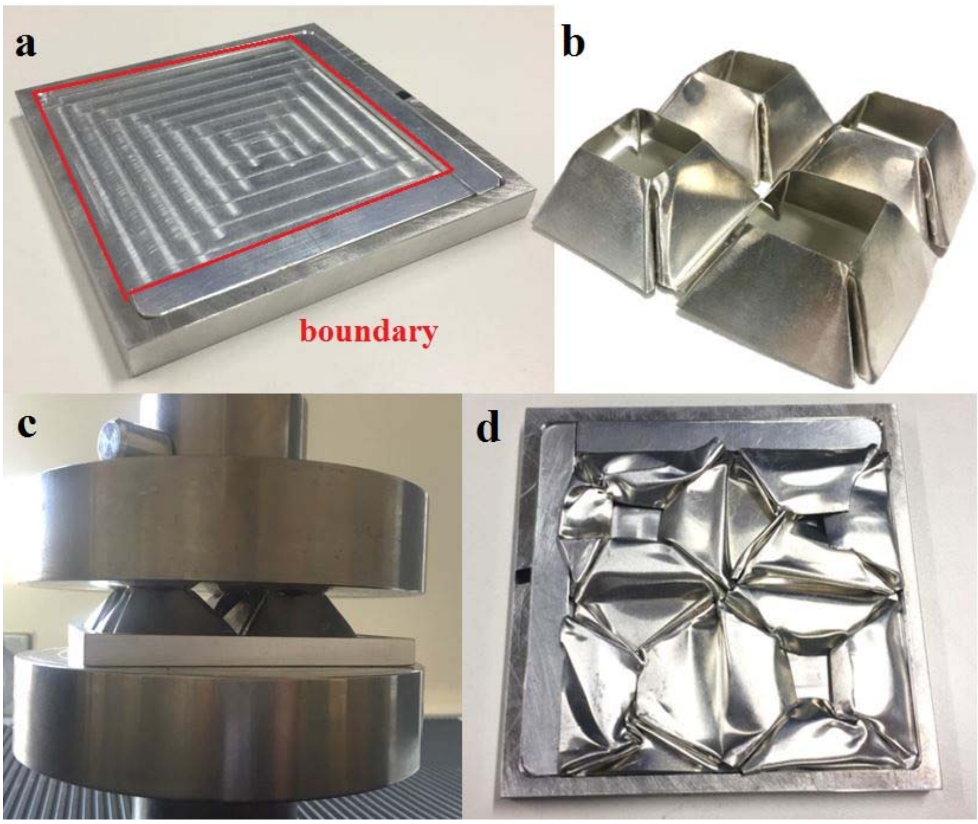

Figure 3. (a) Supporting plate with a 2 mm high boundary strip to constrain in-plane movement of sample; (b) folded SDK sample; (c) quasi-static flatwise crushing test; (d) deformation of the sample after the test

Quasi-static tensile test of the 0.26 mm-thick Aluminium sheet material used for sample folding is also carried out as per the standard ASTM E8M-04 [26] to define the material properties. A loading rate of 0.5 mm/min is applied on the testing specimen. Digital image correlation (2D-DIC) techniques are used in this test to measure the fields of displacements and strains of the specimens. The typical true stress-strain curve of Aluminium strip specimen is shown in Figure 4 (a) and the DIC strain field at the maximum strain is shown in Figure 4 (b). The material testing data is obtained and used in the subsequent numerical simulations.

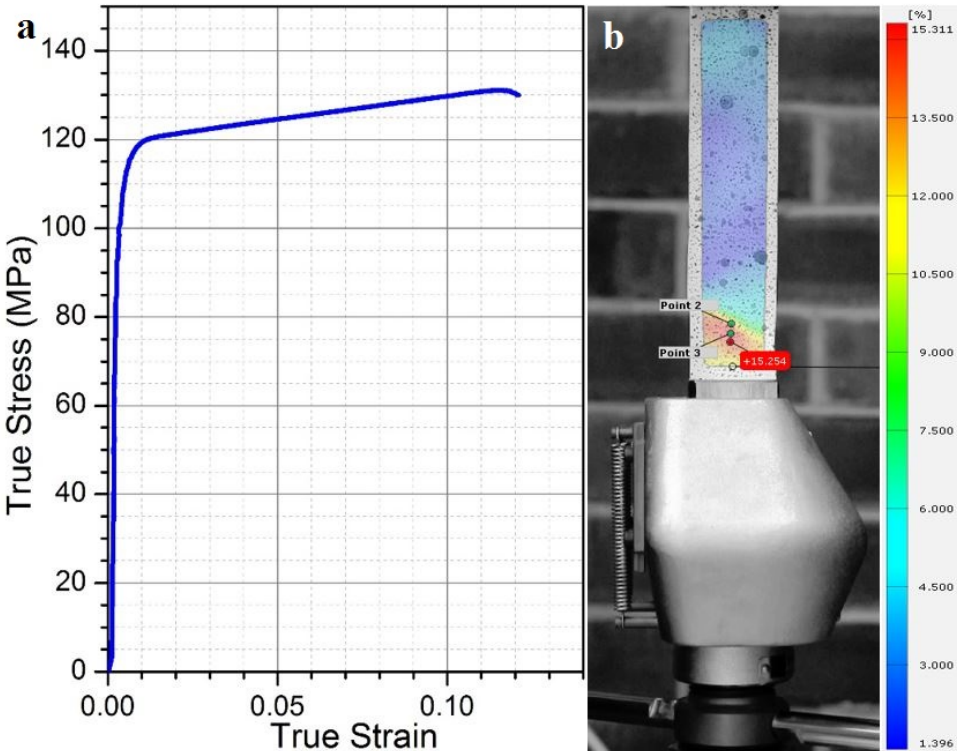

Figure 4. (a) True stress-strain curve of Aluminium 1060 used for folding; (b) DIC image of the Aluminium strip tested at the maximum strain

2.2 Numerical modelling

Finite element software LS-DYNA 971 is used for numerical simulation in this study. The SDK foldcore is constructed by using Belytschko-Tsay type shell element. It is placed between two rigid solid blocks. The top rigid block moves with 0.05 m/s constant crushing speed till around 80% strain. This is because that 1 mm/min quasi-static loading rate used in test is too time consuming for explicit numerical simulation, and 0.05 m/s is found sufficient to simulate accurate quasi-static loading condition in the simulation [19]. Similar to the base plate used in the experiments, bottom plate in the numerical model is also modelled in detail as shown in Figure 5.

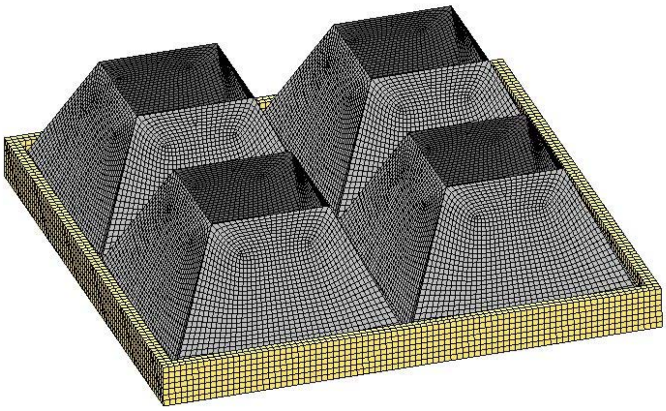

Figure 5. Numerical model of SDK foldcore and the base plate with outer boundary strips

As shown in Figure 4, material properties and true stress-stain data for the sample sheet material Aluminium 1060 are listed in Table 1 and Table 2. Material model *MAT024 PIECEWISE LINEAR PLASTICITY is used. Strain rate effect of aluminium is insignificant [27] and it is therefore not considered in this study. The self-contact of the foldcore during the crushing process is described using keyword * CONTACT AUTOMATIC SINGLE SURFACE, and the contacts between foldcore and top crushing plate/bottom supporting plate are set by using *CONTACT AUTOMATIC NODES TO SURFACE with friction taken into consideration.

Table 1. Material properties of Aluminium 1060

Parameter	**Young's Modulus (GPa)**	**Poisson's ratio**	**Yield stress (MPa)**	**Density (kg/m^3)**
Value	69	0.33	67.7	2710

Table 2. True stress-stain data of Aluminium 1060

Strain	0	0.002	0.005	0.013	0.063	0.121
Stress (MPa)	0	67.7	112.3	120.1	125.8	130.6

2.3 Model calibration

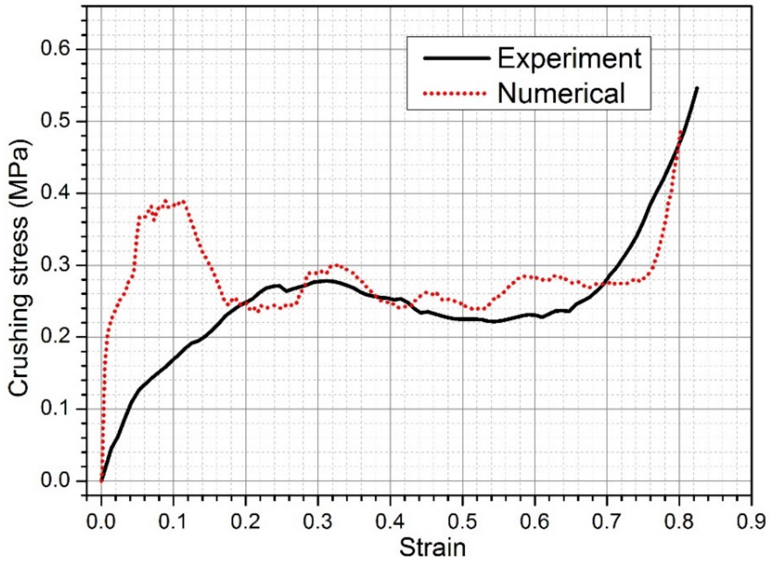

Figure 6. Stress-strain curves of SDK folded sample from both experiment and numerical simulation

As shown in Figure 6, the key criteria including plateau stress and densification strain are similar for the two curves from experiment and numerical simulation. A larger discrepancy of peak crushing stress can be observed between the numerical simulation and experiments. This is caused by the inevitable imperfection of the sample from hand folding process. As mentioned previously, the overall dimension including the height of the sample is slightly larger than the model used in the numerical simulation. Slight gaps and uneven level of adjacent unit cell can be observed in Figure 3 (b) as well. The uneven height of the tested sample resulted in the imperfect contact. In the test, the higher core/edge was in contact with the loading plate before the lower part of the core, and buckled first. This led to the smaller initial stiffness of the core and also smaller crushing stress. Once the entire core was in contact with the loading plate and resisting the load, i.e., in the plateau phase, the numerical result matches the test data well. Similar discrepancy of peak crushing stress between numerical simulation and experiments were also observed in other studies of folded structures such as cube and eggbox kirigami foldcore [19]. Alternative folding method such as stamping could be used in future to improve the folding quality of the core. Similar deformation mode can be also observed in the test and numerical simulation as shown in Figure 3 (d) and Figure 7, respectively. Some sidewalls bend toward the centre. The corners of the foldcore outer sides lift up slightly and the buckling appears along the interconnections in-between sidewalls. However, the deformation in experiment is less symmetric between the unit cells, again because of imperfect folding of the test sample.

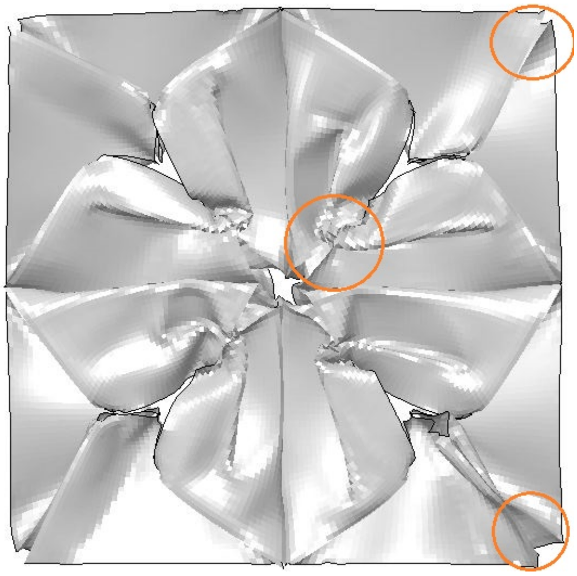

Figure 7. Top view of the deformed SDK foldcore sample at around 0.8 strain

The aim of this study is to exam the potential application of SDK foldcore in sacrificial cladding. Key criteria including initial peak stress, plateau stress and densification strain are used to describe and evaluate the performance. The plateau stress and densification strain between experiment and numerical simulation are in good agreement, indicating similar energy absorption capability. The overestimated peak stress in numerical simulation caused by the perfect geometry of the foldcore will lead to a higher load transmitted to the protected structure than the actual scenario. Therefore, the numerical model slightly overestimates the peak load transmitted to the protected structure with SDK foldcore as sacrificial cladding under blast loading, which indicates conservative prediction from numerical simulation.

3. Performance under various blast loads

3.1 Sacrificial cladding set up

The performance of sacrificial cladding with SDK foldcore as core is evaluated and compared with square honeycomb and aluminium foam in this section. The dimension of unit cell of SDK foldcore is scaled up twice as compared to the tested specimen to have a more reasonable configuration with a 40 mm-thick sacrificial cladding core as shown in Figure 8. The unit cell size of SDK foldcore increases from 40 x 40 x 20 mm used in compression test to 80 x 80 x 40 mm for cladding setup. The square honeycomb is set to have the unit cell dimension of 40 x 40 x 40 mm so it has the same top-opening dimension as SDK foldcore. The same cladding core height of 40 mm is set for aluminium foam as well. The 330 x 330 x 5 mm aluminium plate is used for all three sacrificial claddings as top layer, where the core spaces of these claddings are kept the same as 320 x 320 x 40 mm.

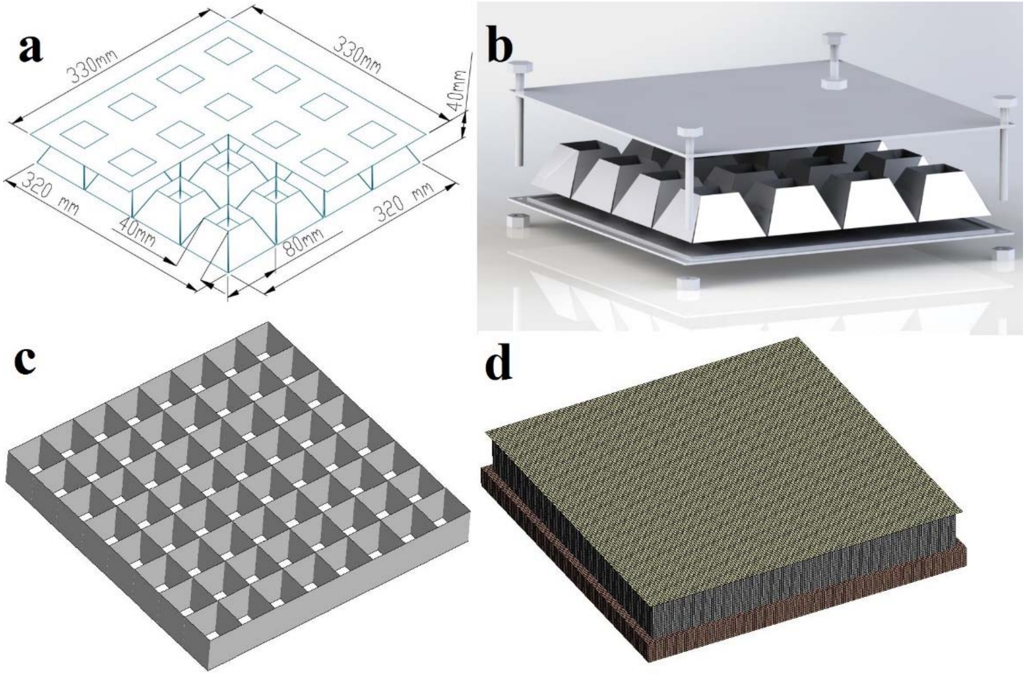

Figure 8. (a) Numerical model of cladding with SDK foldcore as core; (b) proposed assembling of SDK foldcore sandwich structure as sacrificial cladding; (c) square honeycomb core; (d) cladding with aluminium foam core

In this study, blast mitigation performances of sacrificial claddings with different cores are compared by using the criteria including the energy absorption by the core and the peak load transmitted to the protected structure. Therefore, the back skin of the cladding is neglected and the core is placed directly on top of the rigid block as shown in Figure 8 (d). The rigid block is set with density of 2400 kg/m^3 and Young's modulus of 200 GPa [28], modelled by *MAT020 RIGID in LS-DYNA. Similar boundary conditions as in many current cladding studies [28-30] are applied in the model, where sacrificial cladding is simply placed on the surface of structure. For the cladding with aluminium foam core and square honeycomb, the core and top plate are simply supported. The rigid block is fixed in all degree of freedom. The top plate is set to be fixed along the in-plane directions at corners and free to move vertically as shown in Figure 8 (b). No glue or other fixing is applied for all three claddings. For cladding with SDK foldcore, similar to the crushing experiment and numerical model calibration, outer boundary is constructed in the model to constrain the horizontal movements of foldcore outer edges. It should be noted that the interaction between cladding core and the protected structure is neglected in this study to save computational effort. This assumption is believed having insignificant influence on the numerical results because the stiffness of sacrificial cladding is usually substantially smaller than that of the protected structure.

Due to the limitation of aluminium foam fabrication technology, the lowest relative density for aluminium foam is 5% from CYMAT™ [31]. Therefore, the wall thickness for SDK foldcore and square honeycomb is calculated to be 0.94 mm and 0.87 mm respectively to make the relative density of the core the same as 5% aluminium foam for comparison. It is worth noting that the wall thickness of 0.94 mm is only used to match the light aluminium foam with 5% relative density. It is likely to be too thick for the folding process and also leads to the increase of strain rate dependency for cladding structure, which might be a drawback for the application such as sacrificial cladding due to the thickening of vertical triangular interconnections.

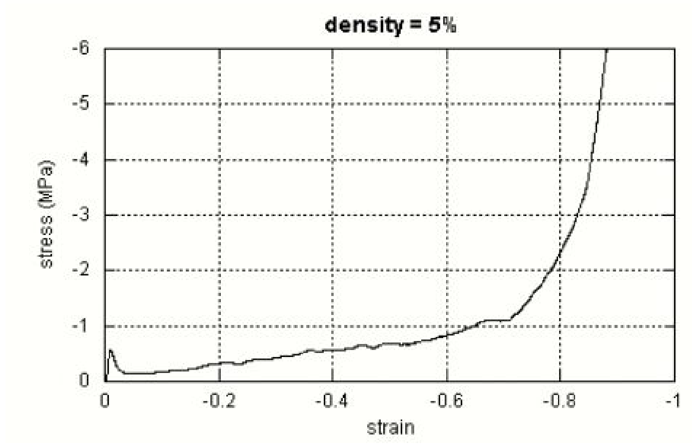

Figure 9. Stress-strain curve of CYMAT closed cell aluminium foam with 5% relative density crushed in out-of-plane direction [31]

The same material model is used for SDK foldcore and square honeycomb by adopting the same material parameters obtained in quasi-static tests and used in numerical simulation. Aluminium foam is modelled by *MAT063 CRUSHABLE FOAM, with stress-strain data found in CYMAT manual as shown in Figure 9 [31], where the strain rate effect for the plateau stress of aluminium foam is not obvious [32] and not included in this numerical study. The Belytschko-Tsay type shell element with material properties given in Table 1 and Table 2 is used for SDK foldcore, square honeycomb and their flat top plates. The same contacts as in the numerical model calibration are used with friction taken into consideration. As shown in Figure 10, mesh convergence test is carried out for aluminium foam cladding model under 1 kg of TNT explosion with 1.5 m stand-off distance. Good agreement can be observed for mesh size of 1 and 2 mm in terms of peak transmitted force and average transmitted force exerted on the protected structure. Therefore 2 mm mesh, which leads to more than half a million elements for the aluminium foam cladding core, is sufficient for the following numerical studies. Mesh size of 2 mm is used for all three models.

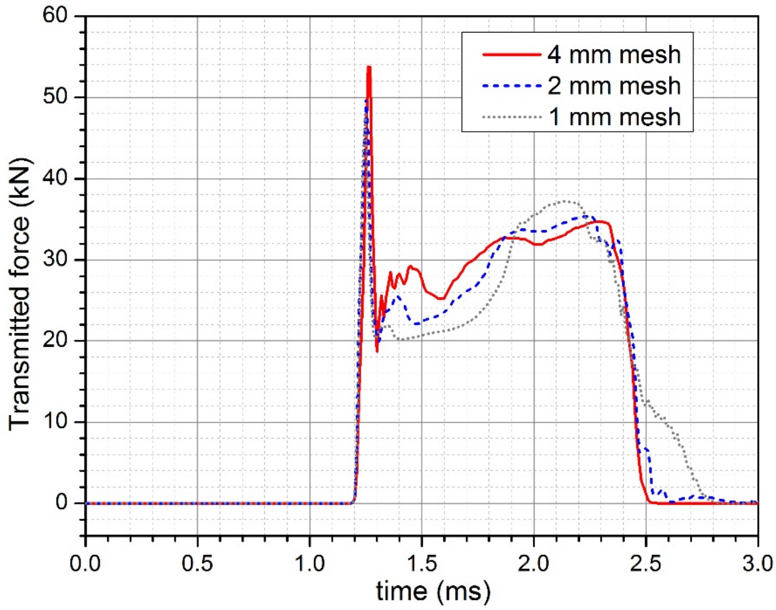

Figure 10. Mesh convergence test for numerical model under 1 kg TNT explosion with stand-off distance 1.5 m

3.2 Structural response comparison

Different blast intensities are simulated with 1, 2, 4 and 6 kg of TNT placed at 1500 mm above the center of the front plate of claddings, in accordance with some previous experiments on the claddings with the stand-off distance of 1 to 2 m [28, 33]. The keyword * LOAD BLAST ENHANCED is used in LS-DYNA. The structure without cladding is also simulated to obtain the force time history for comparison. The stand-off distance for this unprotected structure is 1540 mm, since the cladding has a height of 40 mm.

Table 3. Peak transmitted load, duration, crushed distance at cladding center and energy absorption by core of different cladding configurations under various TNT blast loads

Cladding types		P_{peak} (kN)	$P_{average}$ (kN)	Duration (ms)	Peak crushed distance at centre δ (mm)	Energy absorption by core (J)
1 kg TNT 1.5 m/kg^(1/3)	**Without cladding**	146	-	0.78	-	-
	Square honeycomb	281	44.7	0.78	0.1	2
	Aluminium foam	50	27.9	1.30	9.6	278
	SDK foldcore	120	45.4	0.78	0.6	43
2 kg TNT 1.19 m/kg^(1/3)	**Without cladding**	285	-	0.79	-	-
	Square honeycomb	456	74.1	0.78	0.3	15
	Aluminium foam	75	49.4	1.28	19.9	965
	SDK foldcore	160	83.1	0.75	2.7	318
4 kg TNT 0.95 m/kg^(1/3)	**Without cladding**	562	-	0.80	-	-
	Square honeycomb	652	130	0.78	0.4	167
	Aluminium foam	414	121	0.95	33.3	3070
	SDK foldcore	236	131	0.82	10.9	1910
6 kg TNT 0.83 m/kg^(1/3)	**Without cladding**	831	-	0.79	-	-
	Square honeycomb	676	191	0.74	10.2	1260
	Aluminium foam	1750	247	0.70	36.7	5530
	SDK foldcore	272	170	0.88	17.9	3860

The time history curves of transmitted force to the protected structure with different claddings under various blast loads are shown in Figure 11. When subjected to the blast load of 1 kg TNT, the peak force exerted on structure is around 146 kN for the case without cladding. Force reduction is observed for the aluminium foam and SDK foldcore claddings, whereas the square honeycomb cladding configuration experiences higher peak transmitted load than the case without any protective cladding. Force reduction for cladding with SDK foldcore is not as significant as that with the aluminium foam core for this loading scenario. Similar observations for the case with the blast load of 2 kg TNT can be drawn, i.e., the aluminium foam core results in the largest force reduction, followed by the SDK foldcore claddings, while the protected structure experiences a larger peak load if the square honeycomb cladding is used than unprotected structure. For the scenarios with blast loads of 4 kg and 6 kg, large reduction in transmitted peak force is observed for SDK foldcore. The peak transmitted force to the protected structure with aluminium foam cladding becomes higher than the other two cladding configurations and even higher than the structure without cladding under 6 kg of TNT explosion.

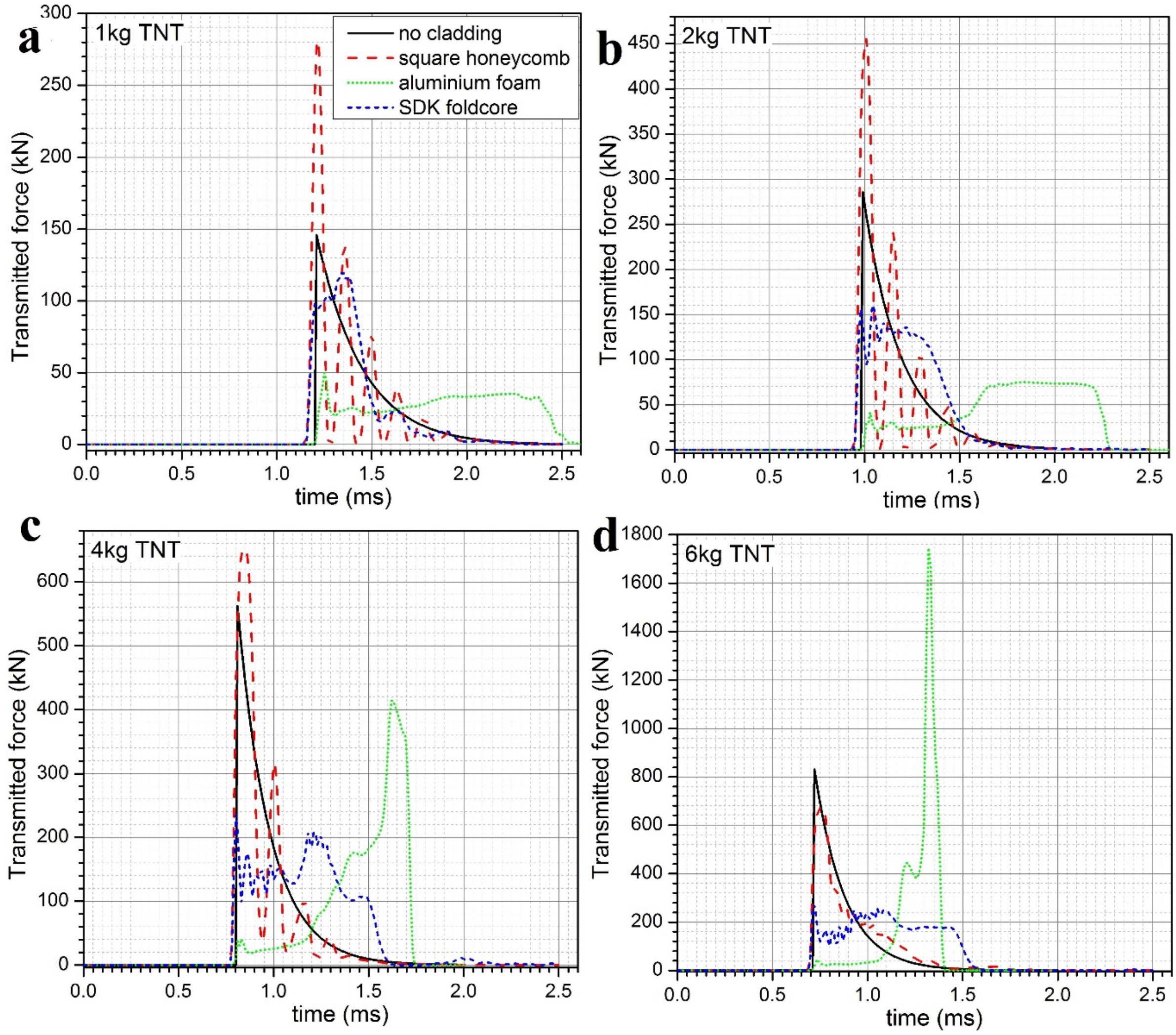

Figure 11. Comparison of transmitted force-time history curves under different blast loads; (a) 1kg TNT; (b) 2kg TNT; (c) 4kg TNT; (d) 6kg TNT; note y-scales are different for each graph

The above observations indicate that the aluminium foam cladding and the square honeycomb cladding have mixed performances, while the performance of SDK foldcore is consistent, i.e., it always leads to a reduction on the peak transmitted force to the protected structure in the blast loading range considered in the study. The mixed performance of the aluminium foam cladding and the square honeycomb cladding is related to their stiffness and strength. The deformation of the cladding includes three states i.e. (1) elastic state, (2) plastic state and (3) fully densified state and all of which are demonstrated in Figure 11. For the structure with SDK foldcore under 1 kg and square honeycomb cladding under 1 kg, 2 kg and 4 kg blast loading, transmitted forces fluctuate multiple times, representing elastic state of the deformation as shown in Figure 11 (a-c). This is because the applied load is relatively small and no significant buckling damage and plastic deformation of the core occur. The core is still primarily in elastic state. This is confirmed by the very small center panel crushed deflections of these two cores as listed in Table 3. Because the core structure remains primarily in elastic stage, it acts like a conduit to transmit the blast load instead of reducing blast load. On the other hand, the aluminium foam cladding is relatively weak and experienced significant crushing failure, which absorbs significant amount of blast energy. Therefore the transmitted load to the protected structure is largely reduced. The second state is the plastic deformation where the impulse from blast wave is fully absorbed by the deformation of the cladding core before it reaches densification, as shown in Figure 12 (a-c). This phenomenon can be observed for the square honeycomb cladding under 6 kg TNT blast loading, the Aluminium foam cladding under 1 and 2 kg TNT explosion and the SDK foldcore cladding under 2, 4 and 6 kg TNT explosions. The third state of core deformation is the full densification of cladding before the end of blast loading, as shown in Figure 12 (d). Full densifications are presented for the aluminium foam cladding under 4 and 6 kg TNT blast loading. Once a cellular core reaches its densification, the stress required for further deformation increases drastically. In some cases, the transmitted load can exceed the blast loading due to the impact of the accelerated fully compacted material onto the protected structure. Similar analysis has been carried out in the study [30] and deteriorating effect of protective cladding has been observed in the experiment [4] as well.

The second state i.e. plastic state is the most effective in energy absorption for the cladding, where the cladding core undergoes plastic deformation and not yet fully compacted during an event of blast. Large amount of energy is dissipated through core deformation and significantly reduces force to be transmitted to the protected structure. Other two states (i.e., elastic state and fully densified state) are caused by too strong or too weak of the cladding core comparing to the reflected blast pressure. The core with lower plateau stress leads to a lower average transmitted load to the protected structure before densification, but it is easier to reach the fully densified state and possibly causes more damage to the protected structure as shown for cladding with aluminium foam under 6 kg TNT blast loading in Figure 11 (c, d) and Figure 12 (d). For the other case (elastic state), it is caused by high crushing resistance of the cladding core or the low value of blast peak pressure, and both of these two causes lead to less effectiveness of the cladding. This can be observed for the cladding with square honeycomb core under 1, 2 and 4 kg TNT blast loading, as shown in Figure 11 (a-c).

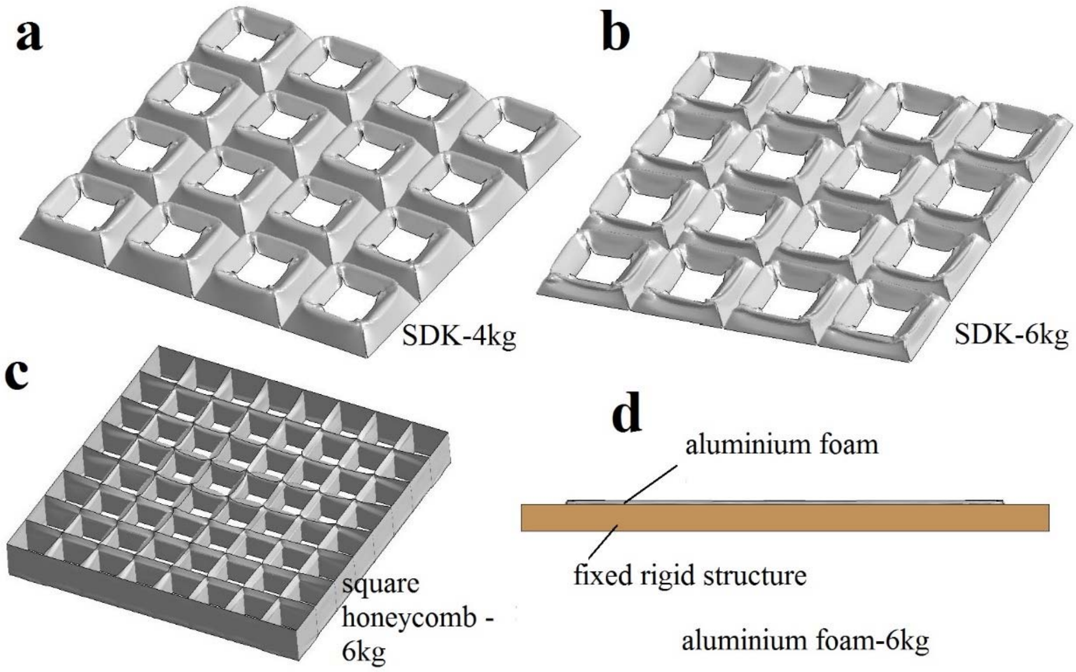

Figure 12. Damage modes of cladding core of (a) SDK foldcore under 4kg TNT blast load; (b) SDK foldcore under 6 kg TNT blast load; (c) square honeycomb under 6 kg TNT blast load; (d) side view of aluminium foam cladding under 6 kg TNT blast load

Overall, the SDK foldcore outperforms the other two cladding configurations by producing a consistent and moderate plateau stress during the whole process of deformation. As shown in Figure 11, SDK foldcore yields much more consistent transmitted load than square honeycomb cladding and a higher plateau stress than the most commonly used cladding material i.e. aluminium foam with the same relative density, which leads to a wider range of applicability of the cladding. However, it is worth noting that the initial peak stress of SDK foldcore is greater than that of aluminium foam with the same density due to the vertical triangular interconnections of SDK foldcore. It was previously studied that the initial peak stress of square honeycomb is in a power relationship with cell wall thickness and it was strain rate dependent due to inertia effect and inertia stabilization effect of the vertical cell walls [34-36]. As mentioned previously, the thickness of SDK cell wall used in this study might be too thick for the folding process and it is only used to match the aluminium foam with the lowest density of 5% available on the market. Therefore, the initial peak stress of SDK foldcore can be greatly reduced by reducing the cell thickness as demonstrated in the previous work where 2.7%

relative density of SDK foldcore was studied [24, 25], and providing similar plateau stress to 5% aluminium foam (Figure 9).

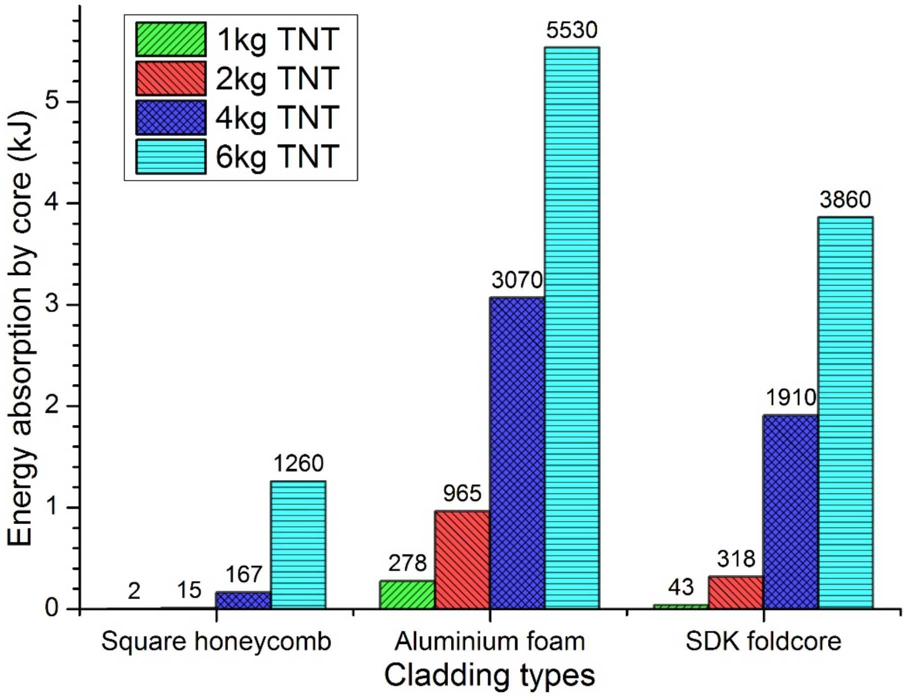

Figure 13. Energy absorption by the core with different cladding configurations and blast loads

Comparisons of energy absorption by the core of the claddings are shown in Figure 13. Energy absorption of each cladding configuration increases with the rising blast load. The low value of square honeycomb foldcore under 1 and 2 kg TNT explosion indicates the elastic state of the core. The aluminium foam cladding has the highest energy absorption capability by the core among these three. The SDK foldcore has lower energy absorption capability than aluminium foam under the same level of blast load. However, as discussed previously, the SDK foldcore has a higher plateau stress and a wider range of applicability of the cladding against different blast loadings comparing with aluminium foam of the same density. It also has a much lower initial peak stress and a more uniform collapsing resistance than the square honeycomb cladding, which demonstrates the superiority of SDK foldcore.

4. Single Degree Of Freedom (SDOF) model

4.1 Analytical model

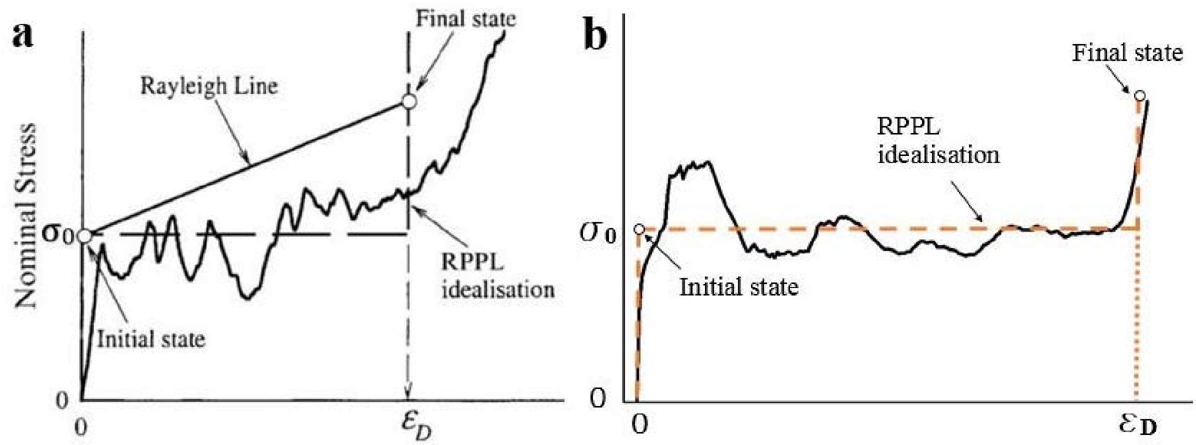

Figure 14. Idealized Rigid-Perfectly Plastic-Locking model for (a) aluminium foam material [37]; (b) SDK foldcore

The SDOF analysis of aluminium foam cladding and the protected main structure was carried out based on shock wave propagation theory in the previous studies [7, 29, 30, 38]. Blast load is simplified as a triangular pulse which follows the form:

$$P(t) = \begin{cases} P_r\left(1-\dfrac{t}{t_0}\right); t \le t_0 \\ 0; t > t_0 \end{cases} \tag{9}$$

where $P(t)$ is the blast pressure at time t, P_r is the initial reflected peak pressure of the blast load and t_0 is the duration of the blast load. As shown in Figure 14 (a), idealized rigid-perfectly-plastic-locking (RPPL) material with a plateau stress of σ_0 [37] is used for aluminium foam cladding in SDOF analysis. Stress-strain curve and idealized RPPL model for SDK foldcore are presented in Figure 14 (b) for comparison. Non-dimensional parameters of foam cladding were then introduced based on cladding properties and blast parameters to evaluate the effectiveness of the foam cladding [30]. It was suggested that the foam cladding should be selected carefully. It is only effective when the impulse from blast load is fully absorbed prior to or at the full densification of the foam cladding. Regions of the effectiveness of foam cladding are divided based on cladding system mechanical parameters and blast loads [30]. In some cases, the foam-protected structure may experience an even larger transmitted load, if the foam is fully densified before the end of the blast impulse. This phenomenon has been recorded in blast test using lightweight polymeric foam as sacrificial claddings [4].

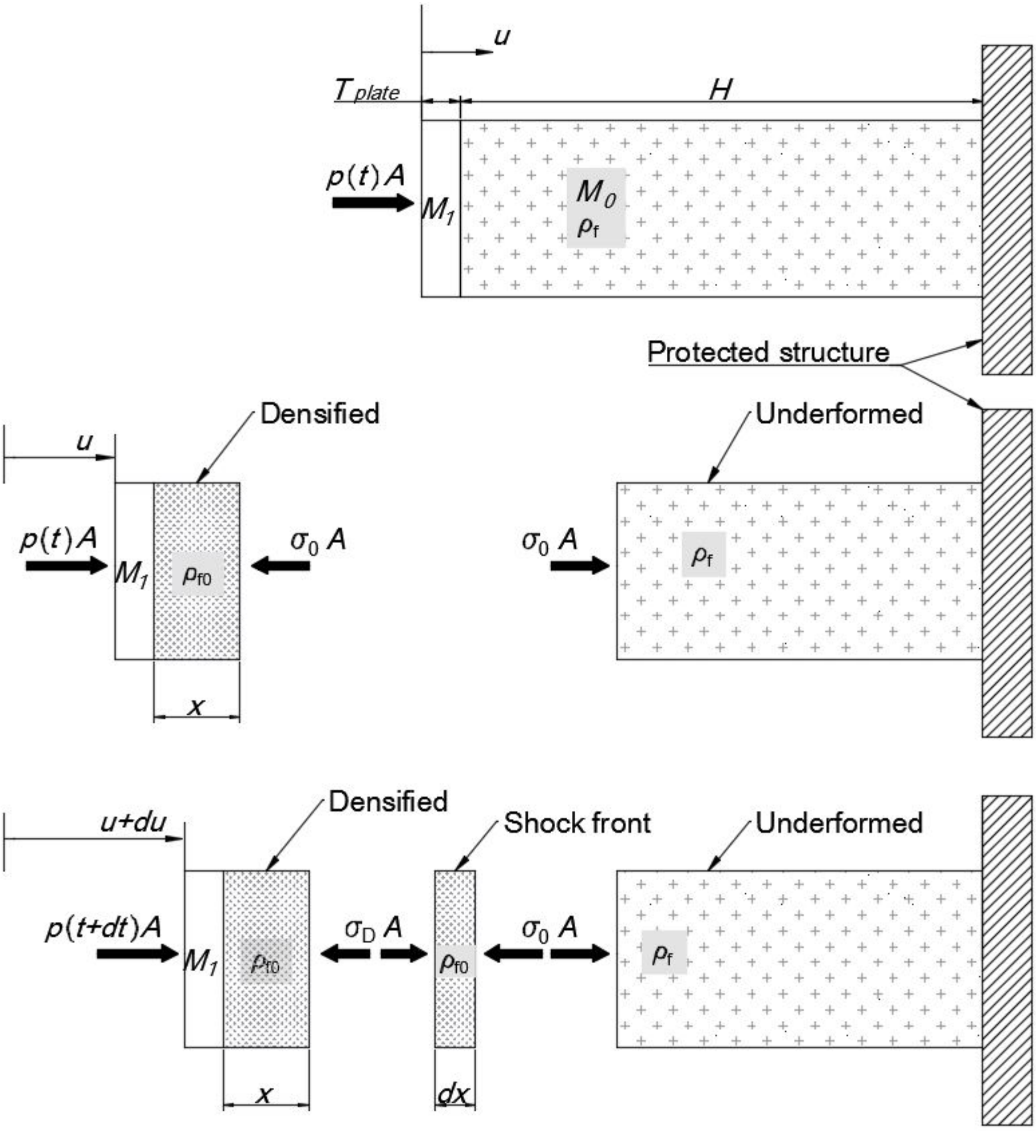

Figure 15. Free body diagrams of aluminium foam cladding system under uniform blast loading at the beginning, time t and t+dt [38]

Free body diagrams of the foam cladding system at *t* and *t*+*dt* are shown in Figure 15, based on the deformation modes observed in the previous experimental study [38]. It is assumed that the foam behind shock front is fully compacted with the same density as base material ρ_{f0}. The compacted zone *x* and the front-panel displacement *u* have the following relationship based on the conservation of mass, where both sides of equation equal to the original length of compacted zone before deforming.

$$\frac{u}{\varepsilon_D} = \frac{x}{1-\varepsilon_D} \tag{8}$$

where ε_D is the densification strain of the foam material ranging between 0 and 1.

The following equation can be obtained by the conservation of momentum of the small compacted foam dx at time t+dt as shown in Figure 15:

$$\rho_{f0} \cdot Adx\left(\dot{u} + d\dot{u}\right) = \left(\sigma_D - \sigma_0\right) Adt \tag{9}$$

where ρ_{f0} is the density of foam base material; A is the cross-section area of the cladding, σ_D and σ_0 are the foam stress immediately behind shock front and foam plateau stress respectively. Similarly, based on the force balance of the front plate and compacted region of foam on the left of element dx:

$$\left[M_1 + \frac{\rho_f A}{1-\varepsilon_D} x\right]\ddot{u} + \left(\sigma_D - P(t)\right) A = 0 \tag{10}$$

where M_1 is the mass of front plate; ρ_f is the foam density; *P(t)* is the blast pressure. Complete solution can be solved from the above equations and a minimum height *H* required to fully absorb blast loading is given as

$$H \geq \frac{I^2}{\left(M_0 + 2M_1\right) P_r A \varepsilon_D} \left[\frac{P_r}{\sigma_0} - \frac{4}{3}\right]; \frac{P_r}{\sigma_0} > 2 \tag{11}$$

where *I* is the total blast impulse and M_0 is the mass of foam cladding.

The crushed distance of the cladding can be expressed as

$$\delta = \frac{I^2}{\left(M_0 + 2M_1\right) P_r A} \left[\frac{P_r}{\sigma_0} - \frac{4}{3}\right]; \frac{P_r}{\sigma_0} > 2 \tag{12}$$

4.2 Displacement comparison with numerical results

Since the SDK foldcore has a similar crushing resistance as aluminium foam, the RPPL material can be assumed for the SDK foldcore as shown in Figure 14, then the SDOF analysis can be applied for simplified calculation of core displacement. The cladding crushed distances are calculated based on the equation (12) and given in Table 4. Since the assumption of the material model in SDOF of cladding system analysis is RPPL, only the responses with aluminium foam and SDK foldcore are calculated due to the relatively low initial peak stress. Furthermore, the equation is derived under the condition that the fully densified state of cladding core is not reached. Aluminium foam becomes fully densified under 4 and 6 kg TNT explosion. Therefore, these two cases are not included in the analysis. The blast parameters P_r and I are taken from numerical simulations of the scenarios without cladding. Other parameters used in equation (12) are calculated by using the dimensions of the foam, plate and their densities.

Table 4. Comparison of centre displacements of numerical (δ_1) and analytical (δ_2) results

	P_r (MPa)	***I (Ns)***	**Aluminium foam**				**SDK foldcore**			
			σ_0 (MPa)	**δ_1 (mm)**	**δ_2 (mm)**	**Difference**	**σ_0 (MPa)**	**δ_1 (mm)**	**δ_2 (mm)**	**Difference**
1 kg TNT	1.34	34.7	0.256	9.6	9.1	-5%	-	-	-	-
2 kg TNT	2.62	57.4	0.457	19.9	14.7	-26%	0.763	2.7	6.5	141%
4 kg TNT	5.16	98.3	-	-	-	-	1.203	10.9	14.0	28%
6 kg TNT	7.63	131.7	-	-	-	-	1.561	17.9	21.2	18%

The results of numerical (δ_1) and analytical (δ_2) predictions are matched well, indicating that the SDOF analysis can be used as a simplified tool to quickly design the cladding configuration. The only large discrepancy (141%) in centre deformation observed between numerical and analytical predictions appear in the cladding with SDK foldcore under 2 kg TNT explosion. This overestimation of the deformation in analytical prediction is caused by the idealized RPPL model, where initial peak of the crushing is not considered and only plastic stage is modelled, as shown in Figure 14. Therefore, under low blast intensities when the deformation of cladding core just reaches the plastic stage, the analytical prediction obtained using SDOF analysis based on perfect plastic deformation assumptions could be overestimated. Furthermore, the deformation and energy absorption of front plate of the cladding system is not considered in this SDOF approach. Thin layer of front plate or cladding with unevenly supported core structure could lead to slight overestimation in this SDOF approach as well. Overall the central displacements analytically predicted by using the above derived formula are in good agreement with the numerical results, indicating the derived formula can be used as a simplified tool to estimate the thickness required for cladding subjected to certain blast loading.

5. Simplified design charts for folded square dome core

As per the equation (11) derived by Hanssen et al [38], the minimum core height *H*, of foam sacrificial cladding is defined by the blast peak reflected pressure P_r, blast impulse *I*, plateau stress of foam σ_0, densification strain ε_D, mass of the front plate M_1 and mass of the foam (cladding core) M_0. However, the mass of the core M_0 is not an independent parameter of the height of the core, *H*. Therefore, Equation (11) for the required core thickness (*H*), previously derived by Hanssen et al [38] is not the complete solution for the designing of the sacrificial cladding. Mass of the core, M_0, and front plate, M_1, are further defined by the density and the size of the core, as given below:

$$M_0 = \rho_f \cdot HA; \tag{13}$$

$$M_1 = n \cdot \rho_f T_{plate} A; \tag{14}$$

where *n* is the ratio between plate density and foam (cladding core) density ρ_f, and T_{plate} is the thickness of the front plate. Substitute equation (13) & (14) into equation (11), it has

$$H \geq \frac{I^2}{\left(\rho_f \cdot HA + 2n \cdot \rho_f T_{plate} A\right) P_r A \varepsilon_D} \left[\frac{P_r}{\sigma_0} - \frac{4}{3}\right]; \frac{P_r}{\sigma_0} > 2 \tag{15}$$

Since all parameters are positive numbers,

$$H^2 + 2n \cdot T_{plate} H \geq \frac{I^2}{\rho_f \cdot P_r A^2 \varepsilon_D} \left[\frac{P_r}{\sigma_0} - \frac{4}{3}\right]; \frac{P_r}{\sigma_0} > 2 \tag{16}$$

$$H \geq \sqrt{\frac{I^2}{\rho_f \cdot P_r A^2 \varepsilon_D} \left(\frac{P_r}{\sigma_0} - \frac{4}{3}\right) + n^2 \cdot T_{plate}{}^2} - n \cdot T_{plate}; \frac{P_r}{\sigma_0} > 2 \tag{17}$$

where blast impulse *I* and blast peak reflected pressure P_r can be obtained from UFC [39]. These two curves are fitted using Matlab as shown in Figure 17. *Z* is the scaled distance, *R* is the stand-off distance and *W* is the equivalent TNT mass in imperial units and to be converted to metric units before submitted into equation (17). Alternatively, fitted curves of reflected pressure (P_r) and impulse (I) in metric units can be found in [40], with the scaled distance ranged from 0.2 to 50 m/kg^1/3.

The fitted equation of the peak reflected blast pressure P_r is given as:

$$P_r = exp\begin{Bmatrix} -0.0084\left[\ln(Z)\right]^5 + 0.0482\left[\ln(Z)\right]^4 + 0.0743\left[\ln(Z)\right]^3 \\ -0.5382\left[\ln(Z)\right]^2 - 2.1322\ln(Z) + 8.8924 \end{Bmatrix}; unit: psi \tag{18}$$

The fitted equation of reflected blast impulse I (i.e. I_r in Figure 17) is given as :

$$\frac{I}{W^{\frac{1}{3}}} = \exp\begin{Bmatrix} -0.00011\left[\ln(Z)\right]^4 - 0.01126\left[\ln(Z)\right]^3 + \\ 0.129\left[\ln(Z)\right]^2 - 1.51731\ln(Z) + 5.4197 \end{Bmatrix}; unit: psi - ms/lb^{1/3}; \tag{19}$$

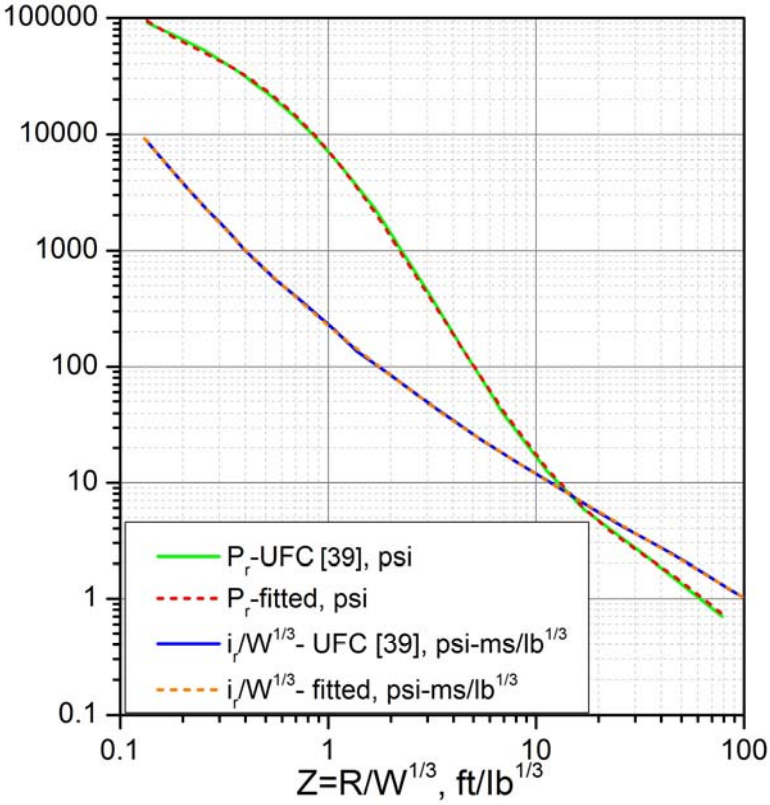

Figure 17. Peak reflected pressure and reflected impulse for a spherical TNT explosion in free air [39] and fitted curves; note: values are read in imperial unit from graph and converted to metric units

These fitted curves have the value of R^2=0.9999 and 1.0000. Good fitting can also be seen from Figure 17. It is noted that all parameters in Figure 17 are in imperial units. The minimum required height of cladding core can then be predicted by equation (17) with any given blast load parameters. These blast loading parameters will be obtained from fitted curves (equation 18&19) in imperial units and converted to metric units for required cladding height calculation. Other parameters of the cladding, such as material, relative density, plateau stress and unit cell size of the SDK folded core are set the same as used in the previous sections.

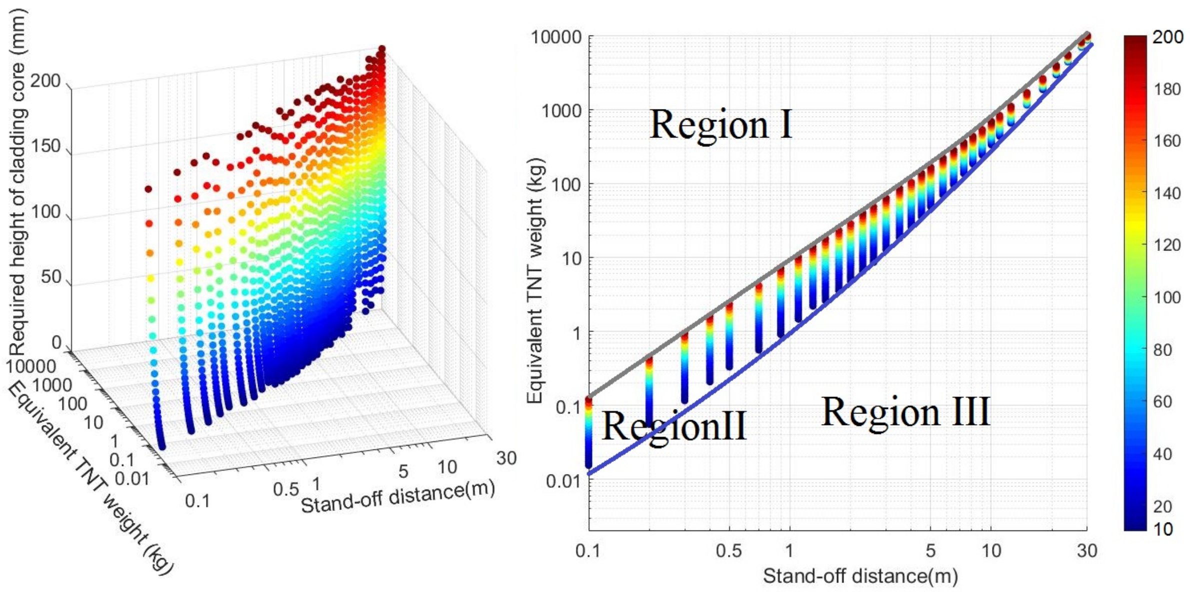

Figure 18. Minimum height of cladding core required at various stand-off distances and blast loads; (L) 3D plot; (R) 2D plot with regions marked out based on performance

A total of around 1,000 calculations of required thickness with different stand-off distances and explosive weights are shown in Figure 18. The front plate thickness is set to be 5 mm made of aluminium with the density of 2700 kg/m^3, cladding core is set to be 5% density of SDK foldcore with a densification strain of 0.7 and a plateau stress of 1.2 MPa which is calculated from average force of SDK foldcore under 2 kg TNT explosion in section 3.2. Such cladding with similar plateau stress has been used for blast protection for RC slab and demonstrated the effectiveness of its blast mitigation capacity [28]. The scaled distance of these blast loading cases, *Z*, is ranged between 0.5 and 3.7 ft/lb^(1/3) (0.2 to 1.46 m/kg^(1/3)), the stand-off distance, *R*, varied from 0.1 m to 30 m, and the equivalent TNT charge weight, *W*, is calculated accordingly. Since this proposed SDK foldcore is a layered structure, the foldcores can be stacked by layers to achieve a larger height. The two blast parameters are manually selected so that the required height of cladding core is within practical range, varying from 10 to 200 mm (equivalent to up to five layers of this SDK foldcore) as shown in the legend in Figure 18. As previously investigated [24], the multi-layered SDK foldcore performs similarly or superior than single layered SDK foldcore under the same blast loading condition, if the interlayer is thick enough and harder to deform than the core.

As expected, the higher blast load or the smaller stand-off distance is, the thicker cladding core is required. The height of cladding core is determined by both blast impulse and peak blast pressure. It is worth noting that the two lines marked out Region II in Figure 18 (R) is roughly the boundary where this type of SDK foldcore would be effective and the region III marked in Figure 18 represents the area of unnecessity of the cladding with this type of SDK foldcore. In other words, under any explosion scenario with the equivalent TNT weight and stand-off distance falls in between the marked two lines (Region II), the structure behind the cladding can be effectively protected by using less than five layers of SDK foldcore. Under such scenario, the pressure transmitted to the protected structure will be greatly reduced to around the plateau stress of the cladding core as compare to the reflected peak blast pressure. For the blast scenario falling in Region III in Figure 18 (R), this cladding will have slight or even no deformation at all, due to the low blast pressure or low impulse. However, this current cladding configuration will not be effective and may cause more damage to the structure behind the cladding for the explosion scenario falling in the region I shown in Figure 18 (R).

This study is based on the proposed geometries of the SDK foldcore with the relative density of 5%. Various geometries, relative density and material configurations including foam infill can be further investigated and their mechanical properties such as plateau stress and densification strain can be obtained. These material and mechanical parameters will affect the performance and the effectiveness of the cladding. They can be used as inputs in this SDOF approach for estimating the required height of core based on the maximum allowable force transmission to the protected structure and the blast load rating during the design phase.

6. Conclusions

The blast mitigation performance of sacrificial cladding with SDK foldcore as core is evaluated and compared with square honeycomb and aluminium foam of the same density. The SDK foldcore demonstrates a rather uniform crushing resistance and a lower initial peak crushing stress under blast loading compared with square honeycomb. This results in an easier initiating of the core deformation and a more efficient blast mitigation capability. Comparing with the aluminium foam, the SDK foldcore of the same mass has a higher average crushing force and a similar consistent collapsing resistance, therefore applicable to wider range of blast intensities. It is worth noting that the thickness of SDK foldcore cell wall can be reduced in order to reduce the initial peak stress during crushing and make it more feasible to fold while maintaining similar plateau stress as aluminium foam of higher density. The cladding performance in general is strongly blast load dependent, sacrificial cladding configurations are required to be selected based on blast loading parameters. Minimum required height of sacrificial cladding core is calculated by using the SDOF analysis of the sacrificial cladding system and the parameters of free air blast from UFC [39]. The height of sacrificial cladding core can be estimated based on the basic cladding material and blast parameters, which could be useful for sacrificial cladding design.

7. Acknowledgement

The authors acknowledge the support from Australian Research Council via Discovery Early Career Researcher Award (DE160101116). Authors also wish to acknowledge the assistance provided by Mr. Pinghe Ni with the curve fitting.

8. References

[1] G. Lu, T. Yu, Energy Absorption of Structures and Materials, Woodhead publishing limited, Cambridge England, 2003.

[2] G.S. Langdon, D. Karagiozova, M.D. Theobald, G.N. Nurick, G. Lu, R.P. Merrett, Fracture of aluminium foam core sacrificial cladding subjected to air-blast loading, International Journal of Impact Engineering, 37, 2010, 638-651.

[3] Z. Xue, J.W. Hutchinson, A comparative study of impulse-resistant metal sandwich plates, International Journal of Impact Engineering, 30, 2004, 1283-1305.

[4] H. Ousji, B. Belkassem, M.A. Louar, B. Reymen, J. Martino, D. Lecompte, L. Pyl, J. Vantomme, Air-blast response of sacrificial cladding using low density foams: Experimental and analytical approach, International Journal of Mechanical Sciences, 128-129, 2017, 459-474.

[5] D. Karagiozova, G.N. Nurick, G.S. Langdon, Behaviour of sandwich panels subject to intense air blasts – Part 2: Numerical simulation, Composite Structures, 91, 2009, 442-450.

[6] G.N. Nurick, G.S. Langdon, Y. Chi, N. Jacob, Behaviour of sandwich panels subjected to intense air blast – Part 1: Experiments, Composite Structures, 91, 2009, 433-441.

[7] C. Wu, Y. Zhou, Simplified analysis of foam cladding protected reinforced concrete slabs against blast loadings, International Journal of Protective Structures, 2, 2011, 351-365.

[8] C. Qi, A. Remennikov, L.-Z. Pei, S. Yang, Z.-H. Yu, T.D. Ngo, Impact and close-in blast response of auxetic honeycomb-cored sandwich panels: Experimental tests and numerical simulations, Composite Structures, 180, 2017, 161-178.

[9] T. Ngo, D. Mohotti, A. Remennikov, Use of polyurea-auxetic composite system for protecting structures from close-in detonations, in: M.G. Stewart, M.D. Netherton (Eds.) 3rd international conference on protective structures, Newcastle, Australia, 2015.

[10] W. Chen, H. Hao, Numerical study of a new multi-arch double-layered blast-resistance door panel, International Journal of Impact Engineering, 43, 2012, 16-28.

[11] W. Chen, H. Hao, Numerical simulations of stiffened multi-arch double-layered panels subjected to blast loading, International Journal of Protective Structures, 4, 2013, 163-188.

[12] W. Chen, H. Hao, Experimental investigations and numerical simulations of multi-arch double-layered panels under uniform impulsive loadings, International Journal of Impact Engineering, 63, 2014, 140-157.

[13] Z. Li, W. Chen, H. Hao, Numerical study of sandwich panel with a new bi-directional Load-Self-Cancelling (LSC) core under blast loading, Thin-Walled Structures, 127, 2018, 90-101.

[14] K. Miura, Zeta-core sandwich-its concept and realization, title ISAS report/Institute of Space and Aeronautical Science, University of Tokyo, 37, 1972, 137.

[15] K. Miura, Method of packaging and deployment of large membranes in space, title The Institute of Space and Astronautical Science report, 618, 1985, 1.

[16] S. Liu, G. Lu, Y. Chen, Y.W. Leong, Deformation of the Miura-ori patterned sheet, International Journal of Mechanical Sciences, 99, 2015, 130-142.

[17] S. Heimbs, Foldcore sandwich structures and their impact behaviour: an overview, in: Dynamic failure of composite and sandwich structures, Springer, 2013, pp. 491-544.

[18] J.M. Gattas, Z. You, The behaviour of curved-crease foldcores under low-velocity impact loads, International Journal of Solids and Structures, 53, 2015, 80-91.

[19] R.K. Fathers, J.M. Gattas, Z. You, Quasi-static crushing of eggbox, cube, and modified cube foldcore sandwich structures, International Journal of Mechanical Sciences, 101-102, 2015, 421-428.

[20] J.M. Gattas, Z. You, Quasi-static impact of indented foldcores, International Journal of Impact Engineering, 73, 2014, 15-29.

[21] T. Nojima, K. Saito, Development of newly designed ultra-light core structures, JSME International Journal Series A Solid Mechanics and Material Engineering, 49, 2006, 38-42.

[22] Z. Li, W. Chen, H. Hao, Numerical study of folded dome shape aluminium structure against flatwise crushing, in: 12th International Conference on Shock & Impact Loads on Structures, Singapore, 2017.

[23] Z. Li, W. Chen, H. Hao, Crushing behaviours of folded kirigami structure with square dome shape, International Journal of Impact Engineering, 115, 2018, 94-105.

[24] Z. Li, W. Chen, H. Hao, Blast resistant performance of multi-layer square dome shape kirigami folded structure,, in: 6th International Conference on Design and Analysis of Protective Structures, Melbourne, Australia, 2017.

[25] H. Hao, Z. Li, W. Chen, Performance of sandwich panel with square dome shape folded kirigami core under blast loading, in: 13th International Conference on Steel, Space and Composite Structures, Perth, Australia, 2018.

[26] ASTM, E8M-04 Standard Test Methods for Tension Testing of Metallic Materials (Metric) 1, ASTM international, 2004.

[27] F. Zhu, L. Zhao, G. Lu, Z. Wang, Structural response and energy absorption of sandwich panels with an aluminium foam core under blast loading, Advances in Structural Engineering, 11, 2008, 525-536.

[28] C. Wu, L. Huang, D.J. Oehlers, Blast Testing of Aluminum Foam–Protected Reinforced Concrete Slabs, Journal of Performance of Constructed Facilities, 25, 2011, 464-474.

[29] G.W. Ma, Z.Q. Ye, Energy absorption of double-layer foam cladding for blast alleviation, International Journal of Impact Engineering, 34, 2005, 329-347.

[30] G.W. Ma, Z.Q. Ye, Analysis of foam claddings for blast alleviation, International Journal of Impact Engineering, 34, 2005, 60-70.

[31] CYMAT, Technical Manual for CYMAT SmartMetal™, CYMAT Technologies Ltd, 2009, 5-1-17.

[32] M.F. Ashby, A. Evans, N.A. Fleck, L.J. Gibson, J.W. Hutchinson, H.N.G. Wadley, Metal foams: a design guide, Materials & Design, 23, 2002, 119.

[33] S. Guruprasad, A. Mukherjee, Layered sacrificial claddings under blast loading Part II—experimental studies, International Journal of Impact Engineering, 24, 2000, 975-984.

[34] Z. Xue, J.W. Hutchinson, Crush dynamics of square honeycomb sandwich cores, International Journal for Numerical Methods in Engineering, 65, 2006, 2221-2245.

[35] J. Zhang, M. Ashby, The out-of-plane properties of honeycombs, International Journal of Mechanical Sciences, 34, 1992, 475-489.

[36] F. Côté, V.S. Deshpande, N.A. Fleck, A.G. Evans, The out-of-plane compressive behavior of metallic honeycombs, Materials Science and Engineering: A, 380, 2004, 272-280.

[37] P.J. Tan, J.J. Harrigan, S.R. Reid, Inertia effects in uniaxial dynamic compression of a closed cell aluminium alloy foam, Materials science and technology, 18, 2002, 480-488.

[38] A. Hanssen, L. Enstock, M. Langseth, Close-range blast loading of aluminium foam panels, International Journal of Impact Engineering, 27, 2002, 593-618.

[39] US Army Corps of Engineers, Naval Facilities Engineering Command. Air Force Civil Engineer Support Agency. Unified Facilities Criteria: Structures to Resist the Effects of Accidental Explosions, in: UFC 3-340-02, 2008.

[40] H. Hao, M.G. Stewart, Z.-X. Li, Y. Shi, RC column failure probabilities to blast loads, International Journal of Protective Structures, 1, 2010, 571-591.